




Cite this: *Org. Biomol. Chem.*, 2017, **15**, 10238

## Prolonged bioluminescence imaging in living cells and mice using novel pro-substrates for *Renilla* luciferase†

Mingliang Yuan,<sup>‡a</sup> Xiaojie Ma,<sup>‡b</sup> Tianyu Jiang,<sup>a</sup> Yuqi Gao,<sup>a</sup> Yuanyuan Cui,<sup>a</sup> Chaochao Zhang,<sup>a</sup> Xingye Yang,<sup>a</sup> Yun Huang,<sup>c</sup> Lupei Du,<sup>a</sup> Iliia Yampolsky<sup>d,e</sup> and Minyong Li <sup>\*a,f</sup>

The prodrug or caged-luciferin strategy affords an excellent platform for persistent bioluminescence imaging. In the current work, we designed and synthesized ten novel pro-substrates for *Renilla* luciferase by introducing ester protecting groups of different sizes into the carbonyl group of the free luciferin **1**. Taking advantage of intracellular esterases, lipases, and nucleophilic substances, the ester protecting groups were hydrolyzed, resulting in the release of a free luciferin and a bioluminescence signal turn-on. Among the tested pro-substrates, the butyryloxymethyl luciferin **7** exhibited low cytotoxicity and a prolonged luminescence signal both *in cellulo* and *in vivo*. Therefore, the butyryloxymethyl luciferin **7** can act as a promising substrate for noninvasive extended imaging in diagnostic and therapeutic fields.

Received 6th July 2017,  
Accepted 16th November 2017

DOI: 10.1039/c7ob01656e

rsc.li/obc

## Introduction

Noninvasive bioluminescence imaging (BLI) for real-time monitoring of biological events in living cells and animals has been widely adopted in both basic research and translation applications, including gene therapy, stem cell tracking, tumor growth assessment, drug development, and probing protein–protein interactions.<sup>1–7</sup> BLI employs luciferases such as *Renilla* luciferase as reporters to generate visible light during the catalytic oxidation of the corresponding luciferins. Compared with fluorescence imaging (FLI), BLI is endowed with many intrinsic advantages including no requirement for excitation light,

negligible background signal, high sensitivity, broad dynamic ranges, superior biocompatibility and versatility in the choices of luciferases and cognate luciferins.<sup>8–13</sup> Therefore, BLI has become an important imaging method for biomedical research.

The two most commonly utilized BLI reporters are *Firefly* luciferase (Fluc, 61 kDa) and *Renilla* luciferase (Rluc, 36 kDa).<sup>14</sup> Fluc can catalyze the oxidation of its natural substrate D-luciferin to produce yellow-green light (540–615 nm) in the presence of O<sub>2</sub>, adenosine triphosphate (ATP), and Mg<sup>2+</sup>. The Fluc/D-luciferin pair has gained wide popularity in cellular and animal imaging given the strong emission signals and biocompatibility.<sup>15</sup> However, the consumption of ATP during the bioluminescence reaction might perturb the metabolic state of cells, thus increasing the experimental complexity. On the other hand, Rluc and coelenterazine (CTZ), only requiring molecular oxygen, constitute an alternative BLI system.<sup>16–19</sup> The Rluc/CTZ pair emits blue-green light with a spectral peak of 475 nm. Moreover, Rluc has been successfully expressed in mammalian cells with good biocompatibility.<sup>20</sup> Aside from being a useful reporter in cellular assays, Rluc/CTZ has the potential for *in vivo* imaging because of its versatility as well as the lack of ATP requirements.<sup>21</sup> Rluc has also been utilized as an energy donor to be paired with the green fluorescent protein (GFP) or its variants as an energy acceptor in bioluminescence resonance energy transfer (BRET) for investigating protein–protein interactions.<sup>22,23</sup> The current BRET systems are mainly divided into BRET<sup>1</sup>, BRET<sup>2</sup>, and eBRET. BRET<sup>1</sup> and BRET<sup>2</sup>, respectively, employ coelenterazine h and

<sup>a</sup>Department of Medicinal Chemistry, Key Laboratory of Chemical Biology (MOE), School of Pharmacy, Shandong University, Jinan, Shandong 250012, China.

E-mail: mli@sdu.edu.cn; Fax: +86-531-8838-2076; Tel: +86-531-8838-2076

<sup>b</sup>Department of Otorhinolaryngology, Qilu Hospital of Shandong University, Jinan, Shandong 250012, China

<sup>c</sup>Centre for Epigenetics and Disease Prevention, Institute of Biosciences and Technology, Department of Molecular and Cellular Medicine, College of Medicine, Texas A&M University, Houston, TX 77030, USA

<sup>d</sup>Shemyakin-Ovchinnikov Institute of Bioorganic Chemistry of the Russian Academy of Sciences, Miklukho-Maklaya, 16/10, Moscow 117997, Russia

<sup>e</sup>Pirogov Russian National Research Medical University, Ostrovitianov 1, Moscow 117997, Russia

<sup>f</sup>State Key Laboratory of Microbial Technology, Shandong University, Jinan, Shandong 250100, China

†Electronic supplementary information (ESI) available: The details of preparation of the luciferin esters and their NMR and HR-MS spectra. See DOI: 10.1039/c7ob01656e

‡These authors contributed equally.



DeepBlueC™ as the Rluc substrate. eBRET utilizes a protected form of coelenterazine h, called EnduRen™, which can be used to monitor protein–protein interactions in real time for up to 6 h.<sup>24</sup> In addition, the Rluc/CTZ system has been applied in the real-time monitoring of reactive oxygen species, gene expression, and neural stem cell transplantations.<sup>25–28</sup>

However, the wide application of the Rluc/CTZ pair is hindered owing to the following factors: Firstly, the chemical stability of CTZ is suboptimal in aqueous solution, with the half-life at 37 °C estimated to be approximately 15 min;<sup>29,30</sup> Secondly, CTZ is also unstable in serum and plasma, resulting in a non-ignorable background signal (autoluminescence);<sup>31</sup> Last but not least, the fast catalytic oxidation of CTZ generates bioluminescence signals that decay rapidly, not conducive to prolonged real-time imaging *in vitro* and *in vivo*.<sup>32</sup> It has been well established that CTZ can be stabilized by introducing protecting groups at the reaction site, the 3-carbonyl position of the imidazopyrazinone moiety, thus temporarily prohibiting its recognition with Rluc. When triggered by specific enzymes or small molecules, the caged luciferins can be converted into free luciferins and then combined with Rluc so as to generate a luminescent signal, thereby leading to a longer half-life and a lower autoluminescence.<sup>15,18</sup> Along this line, some Rluc substrates or probes have been well developed. Jelena Levi *et al.* synthesized four DeepBlueC™ derivatives that displayed the potential for improving the BRET<sup>2</sup> assays with good light signal sustainability.<sup>33</sup> ViviRen™ and EnduRen™, produced by Promega Corporation and containing small protecting groups that can be cleaved by intracellular esterases and lipases, presented longer kinetics and diminished autoluminescence.<sup>34</sup> Eric Lindberg *et al.* designed and synthesized two  $\beta$ -galactosidase recognition probes with  $\beta$ -galactose caging groups, displaying improved kinetic profiles and high signal-to-noise ratios when assayed *in cellulo*.<sup>35</sup> Recently, a caged furimazine was developed as the pro-substrate for an engineered luciferase NanoLuc to enable live tissue imaging.<sup>36</sup> Altogether, the caged-luciferin strategy affords an excellent platform for persistent bioluminescence imaging.<sup>37–41</sup>

In previous work, we described a sulfur-containing CTZ analogue **1** with an improved light signal compared to DeepBlueC™.<sup>42–44</sup> The synthesis of the analogues with a sulfur heteroatom was performed from 2-aminopyrazine based on the Suzuki coupling reaction. Key pyrazine intermediates were obtained by reaction of bromo derivatives with the thiol in dry DMF with sodium hydride as the base. The final step of the convergent synthesis of the coelenterazine analogues was achieved by condensation of intermediates, with a diethoxy derivative in ethanol with concentrated HCl. The sulfur heteroatom replacement of the methylene bridge in DeepBlueC™ leads to a bathochromic shift in the bioluminescence reaction with Rluc. The bioluminescence spectra exhibited a significant red-shift (36 nm) for free luciferin **1** compared to DeepBlueC™. As the closer to red the better, the shift toward red is of great interest *in vivo*. Based on this, we designed and synthesized ten novel pro-substrates for *Renilla* luciferase by introducing ester protecting groups of different sizes into the

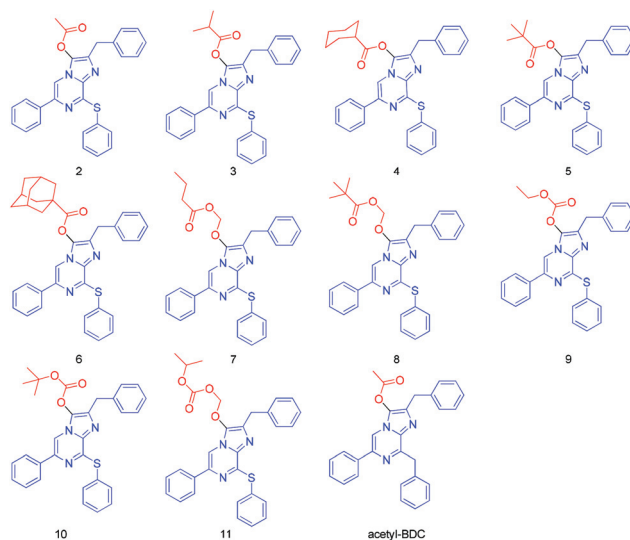


Fig. 1 Chemical structures of prolonged bioluminescent pro-substrates.

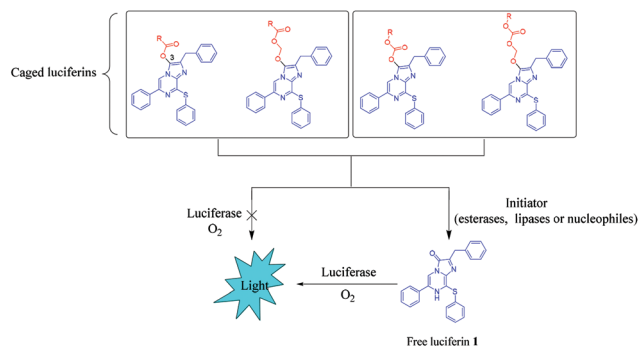
carbonyl group of the free luciferin **1** (Fig. 1). Compounds **2–8** have a carboxylic ester group and the others are luciferin carbonic esters. Upon cell uptake, these prodrug-inspired luciferin derivatives, termed luciferin esters, could be hydrolyzed by intracellular esterases, lipases, and nucleophilic substances to slowly release the free luciferin **1**. Subsequently, a catalytic luciferin–luciferase reaction was activated, thereby resulting in the production of light with a longer half-life and lower background noise (Scheme 1). To demonstrate this hypothesis, we firstly investigated the stability of the luciferin esters in aqueous solution and then performed imaging studies by using a cooled charge coupled-device (CCD) detector in living cells and mice. Of the ten luciferin esters, three compounds can produce detectable signals even after 24 h exposure to the cells. Indeed, the butyryloxymethyl luciferin **7** was of low cytotoxicity and displayed sustained luminescence signals that last >24 h *in cellulo* and *in vivo*. Therefore, the butyryloxymethyl luciferin **7** can serve as a promising long-term bioluminescence imaging probe.

## Results and discussion

### Stability assay

We investigated the stability of the luciferin derivatives in aqueous solution by HPLC and UV analysis. As shown in Fig. 2B and C, the peak at 19.28 min assigned to the luciferin acetyl ester **2** decreased significantly. A new peak belonging to the free luciferin **1** at 10.66 min appeared remarkably. It indicated that the luciferin acetyl ester **2** was extremely unstable, and was easily hydrolyzed to release the free luciferin **1**. Then the obtained data were analyzed by using GraphPad Prism 5.0 software. As the first order reaction is characterized by a  $\ln c-t$  plot, the half-life is independent of the initial concentration and inversely proportional to the rate constant. The half-life





**Scheme 1** Design strategy for prolonged bioluminescent pro-substrates that are compatible with *Renilla* luciferase.

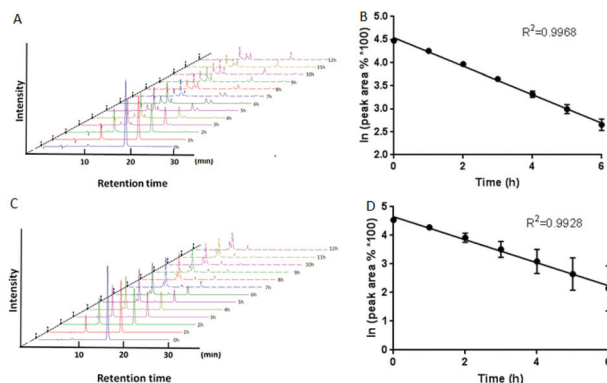


**Fig. 2** *In vitro* stability study of the luciferin esters: (A) HPLC analysis over time (compound 2); (B) HPLC dynamics data analysis for the first 6 hours (compound 2); (C) HPLC analysis over time (compound 10); (D) HPLC dynamics data analysis for the first 6 hours (compound 10).

for the luciferin acetyl ester 2 was determined as 2.25 h under the first-order conditions and the apparent rate constant  $k = (0.3084 \pm 0.007868) \text{ h}^{-1}$ . When subjected to UV analysis, the calculated half-life of the luciferin acetyl ester 2 was 2.80 h (270 nm) and 2.59 h (358 nm), which was almost consistent with that obtained by HPLC (Fig. S1†). In addition, the hydrolysis process of the luciferin isobutyryl ester 3 (Fig. S2A and B†) also belonged to the first-order reaction:  $k = (0.0564 \pm 0.0008645) \text{ h}^{-1}$ ,  $t_{1/2} = \ln 2/k = 12.29 \text{ h}$  (Fig. S2†). So did the carboxylic ester 4 (Fig. S2C and D†):  $k = (0.008899 \pm 0.0006395) \text{ h}^{-1}$ ,  $t_{1/2} = \ln 2/k = 77.89 \text{ h}$ ; compound 5 (Fig. S2E and F†):  $k = (0.004157 \pm 0.001384) \text{ h}^{-1}$ ,  $t_{1/2} = \ln 2/k = 166.74 \text{ h}$ ; compound 6 (Fig. S2G and H†):  $k = (0.01079 \pm 0.004182) \text{ h}^{-1}$ ,  $t_{1/2} = \ln 2/k = 64.24 \text{ h}$ ; carbonic ester 9 (Fig. S2N and M†):  $k = (0.04267 \pm 0.001234) \text{ h}^{-1}$ ,  $t_{1/2} = \ln 2/k = 16.24 \text{ h}$ ; carbonic ester 10 (Fig. 2C and D):  $k = (0.4025 \pm 0.01534) \text{ h}^{-1}$ ,  $t_{1/2} = \ln 2/k = 1.72 \text{ h}$ ; carbonic ester 11 (Fig. S2O and P†):  $k = (0.005784 \pm 0.0007733) \text{ h}^{-1}$ ,  $t_{1/2} = \ln 2/k = 119.84 \text{ h}$ ; for carboxylic ester derivatives 4, 5, 6 with large steric hindrance and carbonic esters 9, 10, 11, we found that they were fairly stable and almost did not undergo hydrolysis. Therefore, we concluded that the hydrolysis process of the luciferin carboxylic esters was commensurate with the

characteristics of the first-order reaction, and that the stability of the luciferin derivatives depends on the size of the protecting group. The butyryloxymethyl luciferin 7 (Fig. S2I and J†) was also commensurate with the characteristics of the first-order reaction, as  $k = (0.006972 \pm 0.0006517) \text{ h}^{-1}$ ,  $t_{1/2} = \ln 2/k = 99.42 \text{ h}$ . *t*-Butyryloxymethyl luciferin 8 (Fig. S2K and L†) had almost no hydrolysis under the same conditions. Collectively, the size and the type of the protecting group and the solubility seem to govern the stability of the luciferin esters in aqueous solution.

### Ionic effect

Considering the effect of inorganic ions on the stability in aqueous solution, we treated the luciferin esters with various representative cations ( $\text{NH}_4^+$ ,  $\text{Mg}^{2+}$ ,  $\text{Ca}^{2+}$ ,  $\text{Fe}^{2+}$ ,  $\text{Fe}^{3+}$ ,  $\text{Cu}^{2+}$ ,  $\text{Al}^{3+}$ ,  $\text{Mn}^{2+}$ ,  $\text{Pb}^{2+}$ ,  $\text{Hg}^{2+}$ ,  $\text{Zn}^{2+}$ ) and anions ( $\text{CH}_3\text{COO}^-$ ,  $\text{HCO}_3^-$ ,  $\text{HSO}_3^-$ ,  $\text{H}_2\text{PO}_4^-$ ,  $\text{S}^{2-}$ ,  $\text{N}_3^-$ ,  $\text{SCN}^-$ ,  $\text{I}^-$ ,  $\text{BO}_3^{2-}$ ,  $\text{S}_2\text{O}_3^{2-}$ ). As shown in Fig. 3, we can see that the above ions induced little or negligible luminescence alterations. Besides some inorganic salts, there are many nucleophilic substances such as reactive sulfur species (glutathione, cysteine, homocysteine *etc.*) in the complex cellular environments. In general, these nucleophilic substances can accelerate the hydrolysis of the luciferin esters. Hence we did not perform further research. Overall, the results indicated that inorganic ions had little impact on the stability of the luciferin esters in aqueous solution, which is critical for their potential application in biomedical imaging.

### Cytotoxicity test

The luciferin esters as imaging agents should have the characteristic of low cytotoxicity. Therefore, the cell viability was investigated by sulphorhodamine B (SRB) assays. After incubation with varying concentrations of luciferin esters for 24 h, no marked cytotoxicity was observed and the  $\text{IC}_{50}$  values of these luciferin esters were much greater than the concentration (40  $\mu\text{M}$ ) used in cell imaging, demonstrating good biocompatibility with live cells (Table S1†). Therefore, we plan to further investigate the feasibility of luciferin esters for imaging in living systems.

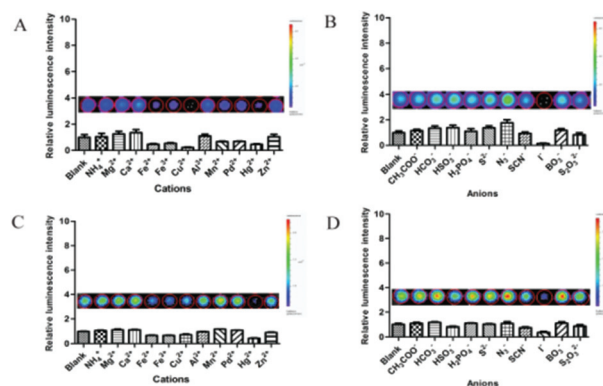


**Fig. 3** Effects of various inorganic ions on the stability of representative luciferin esters 2 (A and B) and 9 (C and D) in aqueous solution.





### Real-time imaging in live cells

To explore whether the luciferin esters can serve as a long-term tracking tool, we firstly performed real-time imaging experiments at the cellular level. ES-2 cells stably expressing *Renilla* luciferase were treated with the luciferin esters and then the light signal was recorded every five minutes. From the kinetics of the bioluminescence (Fig. 4A), the unprotected luciferin **1** displayed rapid luminescent signal decay and lost approximately 80% of its initial light intensity at 10 min. The luciferin acetyl ester **2** easily hydrolyzed by cellular esterases exhibited a maximum light signal at 2 min and then descended rapidly. By contrast, other luciferin esters showed a longer time to peak and slower kinetics owing to the bulkier protecting groups. As for the signal half-life when the initial light intensity falls by half, every compound almost has a half-life period of more than 1 h except for the acetyl ester **2** (Fig. 4A and Fig. S3†). Moreover, of the ten luciferin esters, there were three compounds (**6**, **7** and **8**) with the observable signal after 24 h exposure to the cells (Fig. 4B). However, the light intensity of luciferin esters was inevitably reduced. The corresponding solution to improve the light signal is to simply increase the concentration of the substrates. In addition, the luciferin derivatives with the carbonate structure were unstable in aqueous solution and they showed poor luminescence properties at the cellular level, so we did not carry out further

study for such compounds. Significantly, the butyryloxymethyl luciferin **7** displayed wonderful light signal sustainability. The peak was observed at 15–20 min and remained stable for more than 4 hours. Besides the light intensity of the butyryloxymethyl luciferin **7** was relatively high. Therefore, we chose this compound for imaging of small living animals to further validate its utility *in vivo*.

### *In vivo* imaging

Based on the above-mentioned results, *in vivo* real-time and long-term tumor imaging was further explored. At present, there are few reports of coelenterazine derivatives applied *in vivo*, because such substrates can be oxidized by some substances such as serum and produce background signals. In addition, coelenterazine derivatives can be rapidly and irreversibly catalyzed by *Renilla* luciferase, so that the resulting signal cannot last long. In order to demonstrate that our luciferin esters can serve as a long-term imaging tool *in vivo*, we established a subcutaneous xenotransplanted tumor model of ES-2-Rluc cells in nude mice. When the anesthetized mice were administered intraperitoneally the free luciferin **1** or butyryloxymethyl luciferin **7**, a high autoluminescence signal in the abdominal area was observed. At the same time, the subcutaneous tumors showed weak luminescence (images not shown). Hence the compounds were then injected directly into the tumor site. As shown in Fig. 5A and S4,† the luminous intensity peaked at 15 min after the free luciferin **1** injection and then declined at a faster rate over 2 h. In contrast, the luciferin esters exhibited improved kinetics of the luminescence reaction. Although the signal of the pivaloyloxymethyl luciferin **8** reached a plateau after 20 min, the relatively weak intensity decreased by half at 2 h. While the butyryloxymethyl luciferin **7** had a half-life period of more than 2 h and reached its maximum at 25 min. Surprisingly, the light signal of the butyryloxymethyl luciferin **7** could be detected after 24 h (Fig. 5B). The *O*-acetylated bisdeoxy coelenterazine acetyl-BDC was used as a control in order to compare the strength of the bioluminescence signal *in vivo*. The light intensity reached the peak during 5 minutes. After that, the signal dropped rapidly. The rate of maximum light was lower than that of compounds **1**, **7** and **8**. As shown in Fig. 5A, acetyl-BDC reached its maximum intensity in a short time, but the duration was short, and the bioluminescence intensity was almost impossible to capture after 1 h.

Subsequently, we evaluated the bioluminescence imaging potential of compounds **1**, **7** and **8** in a xenografted mouse model. The intensity of the butyryloxymethyl luciferin **7** was weaker as expected because the free luciferin **1** was released from the butyryloxymethyl luciferin **7**. This indicated that the butyryloxymethyl luciferin **7** was hydrolyzed at a slower rate, so it is more suitable for long-time and stable imaging study. Taken as a whole, our studies demonstrated that the butyryloxymethyl luciferin **7** is a promising long-acting imaging substrate *in vivo*.

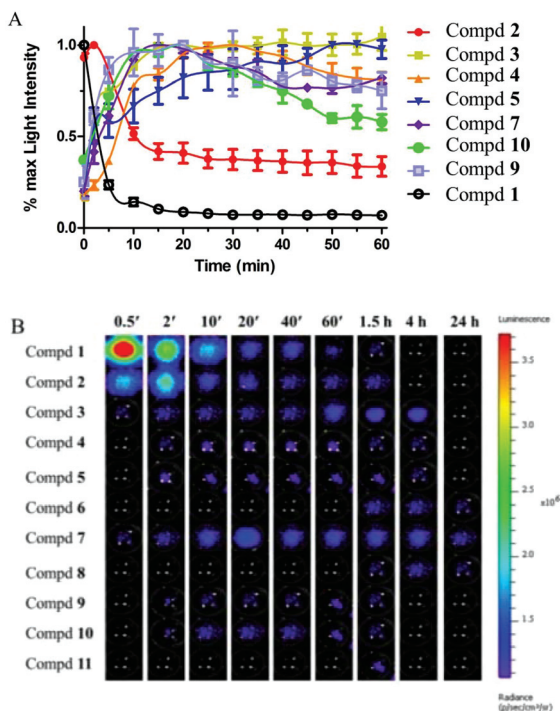


**Fig. 4** ES-2-Rluc cell imaging: (A) the rate of the bioluminescence reaction for the free luciferin **1** and the luciferin esters evaluated as the change of the maximum light intensity in the cell over time; (B) representative bioluminescence imaging for the free luciferin **1** and the luciferin esters in the cell over time.



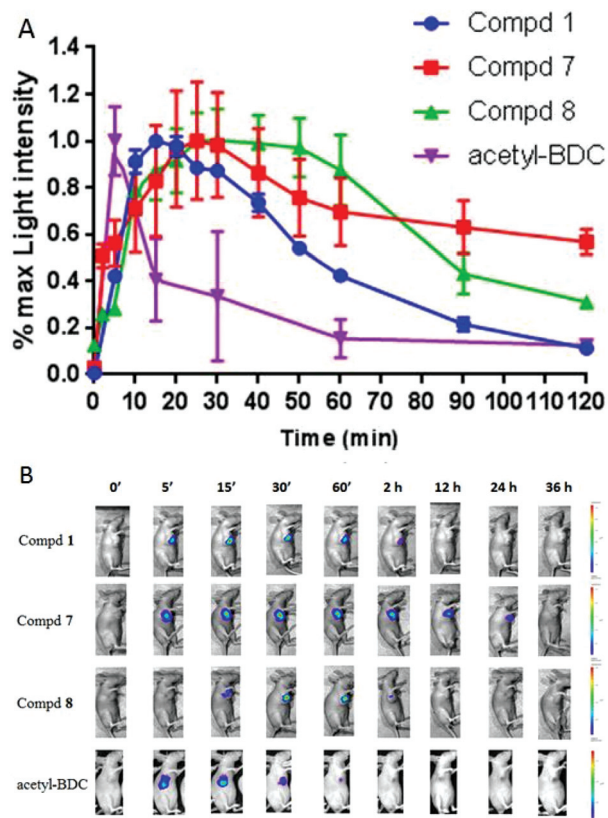


**Fig. 5** *In vivo* imaging: (A) the rate of the bioluminescent reaction for the free luciferin **1** and the luciferin esters evaluated as the change of the maximum light intensity *in vivo* over time; (B) representative bioluminescence imaging for the free luciferin **1** and the luciferin esters *in vivo* over time.

## Experimental

### Materials and apparatus

All chemicals were purchased from commercial suppliers and used without further purification. Ultrapure water was purified with a Mill-Q filtration system. UV-visible absorbance spectra were obtained on a PUXI TU-1901 spectrophotometer. High-pressure liquid chromatography (HPLC) spectra and the purity of the compounds were determined by analytical reverse-phase HPLC (Agilent, 1200 Infinity) on a Phenomenex C-18 column (250 × 4.6 mm). The pH test was performed using a pH-meter (OHAUS, STARTER3100). Melting points were measured using a Mel-Temp apparatus and were not corrected.  $^1\text{H}$  and  $^{13}\text{C}$  NMR spectra were obtained using Bruker AV-300 or AV-600 spectrometers. Mass spectral analyses were performed on an API 4000 (ESI-HRMS).

*Renilla* luciferase was supplied by RayBiotech. ES-2-Rluc cells (a human ovarian cancer cell line stably expressing *Renilla* luciferase) were purchased from Shanghai BioDiagnosis Co., Ltd. Female nude mice (BALB/cA-nu) were purchased from the Animal Center of China Academy of Medical Sciences (Beijing, China). Luminescence imaging was recorded using an IVIS Kinetic (Caliper Life Sciences, USA)

equipped with a cooled charge-coupled device (CCD) camera. Circular specified regions of interest (ROIs) were drawn over the areas, and the total flux was calculated using the Living Image software version 4.0 (Caliper Life Sciences).

### Synthesis

The free luciferin **1** was synthesized according to our previous work.<sup>42</sup> In this paper, we prepared a total of ten luciferin esters by simple esterification or etherification. Note that the free luciferin is unstable, so the reactions should be isolated from air. The detailed synthesis protocols and structural characterization are presented in the ESI.†

### Stability in aqueous solution

The stability of the free luciferin **1** and the luciferin esters was monitored by analytical HPLC and UV. For HPLC analysis, a reverse phase HPLC column from Phenomenex (C18, 250 mm × 4.6 mm) was used. Absorbance was monitored at 276 and 335 nm. The mobile phase was 60% acetonitrile in  $\text{H}_2\text{O}$  containing 0.1% trifluoroacetic acid. The flow was 1.0 mL  $\text{min}^{-1}$  and the injection volume was 20.0  $\mu\text{L}$ . All compounds were dissolved in Tris-HCl buffer (50 mM, pH = 7.4)–methanol (2 : 3, v/v) at a final concentration of 60  $\mu\text{M}$ . The samples were incubated at room temperature and measured at an interval of 1 h. When subjected to UV analysis, all compounds were also dissolved in Tris-HCl buffer (50 mM, pH = 7.4)–methanol (2 : 3, v/v) at a final concentration of 60  $\mu\text{M}$ . Samples for absorption measurements were analysed using a sealed cuvette at room temperature. At appropriate time intervals, absorbance spectra were obtained on a PUXI TU-1901 spectrophotometer against blank solution. All kinetic experiments were performed in duplicate with similar results.

### Ionic effects

Luminescence assays were performed with a cooled charge-coupled device (CCD) camera. Various inorganic ions, including  $\text{NH}_4^+$ ,  $\text{Mg}^{2+}$ ,  $\text{Ca}^{2+}$ ,  $\text{Fe}^{2+}$ ,  $\text{Fe}^{3+}$ ,  $\text{Cu}^{2+}$ ,  $\text{Al}^{3+}$ ,  $\text{Mn}^{2+}$ ,  $\text{Pb}^{2+}$ ,  $\text{Hg}^{2+}$ ,  $\text{Zn}^{2+}$ ,  $\text{CH}_3\text{COO}^-$ ,  $\text{HCO}_3^-$ ,  $\text{HSO}_3^-$ ,  $\text{H}_2\text{PO}_4^-$ ,  $\text{S}_2^-$ ,  $\text{N}_3^-$ ,  $\text{SCN}^-$ ,  $\text{I}^-$ ,  $\text{BO}_3^-$  and  $\text{S}_2\text{O}_3^{2-}$ , were dissolved in 50 mM Tris-HCl buffer (pH = 7.40) up to a concentration of 2 mM. *Renilla* luciferase (2  $\mu\text{g mL}^{-1}$ ) and the luciferin esters (80  $\mu\text{M}$ ) were also diluted with the same Tris-HCl buffer. The detailed procedure is as follows: a volume of 50  $\mu\text{L}$  of luciferin esters was added to an equivalent volume of various ions and incubated at 25 °C for 30 min in a black 96-well plate. After adding 100  $\mu\text{L}$  of *Renilla* luciferase, the bioluminescent signal was immediately recorded with an exposure time of 30 s. As a blank control, Tris-HCl buffer without inorganic ions was added under the same experimental conditions. The experiment was carried out three times with similar results.

### Cytotoxicity test

Sulphorhodamine B (SRB) dye was used to determine the *in vitro* cytotoxicity of the luciferin esters towards ES-2 cells. After the cells ( $10^4$  per well) were incubated in 96-well plates overnight, the culture medium was removed, and serial



dilutions of the luciferin esters (0  $\mu\text{M}$ , 22.5  $\mu\text{M}$ , 45  $\mu\text{M}$ , 90  $\mu\text{M}$ , 180  $\mu\text{M}$ , 360  $\mu\text{M}$ , 720  $\mu\text{M}$ , and 1.44 mM) in complete growth medium were added. The following standard procedure is described in ref. 41. Finally, a microplate reader (BMG, POLARstar® Omega) was used to record the absorbance signal at 540 nm. All the assays were performed in triplicate.  $\text{IC}_{50}$  values of the luciferin esters were calculated using non-linear regression analysis in the Prism 5.0 GraphPad software.

### Real-time imaging in live cells

ES-2-Rluc cells were cultured in Dulbecco's modified Eagle's Medium (DMEM) supplemented with 10% Fetal Bovine Serum (FBS) and 0.5  $\mu\text{g mL}^{-1}$  puromycin. All compounds were dissolved in DMEM (containing 0.1% F-127, no Fetal Bovine Serum) to a gradient concentration (0, 5  $\mu\text{M}$ , 10  $\mu\text{M}$ , 20  $\mu\text{M}$ , 40  $\mu\text{M}$ , 60  $\mu\text{M}$ , 80  $\mu\text{M}$ , and 100  $\mu\text{M}$ ). One night before imaging experiments, ES-2-Rluc cells were seeded in a 96-well culture plate ( $4 \times 10^4$  cells per well). After the medium was removed and cells were washed with DMEM, ES-2-Rluc cells were treated with 100  $\mu\text{L}$  of various concentrations of compounds. Luminescence signals were immediately recorded every 5 min with an exposure time of 100 s. We conducted the experiments in triplicate with similar results.

### In vivo imaging

All animal studies were approved by the Ethics Committee and IACUC of Cheeloo College of Medicine, Shandong University, and were conducted in compliance with European guidelines for the care and use of laboratory animals. The subcutaneous xenotransplanted tumor model in nude mice was established following a reported approach.<sup>8</sup> 5-Week-old female nude mice (BALB/cA-nu) were purchased and group-housed in a room maintained at 25  $^{\circ}\text{C}$  with 40–60% humidity. A total of  $5 \times 10^7$  ES-2-Rluc cells were implanted subcutaneously in the right armpit region of each mouse. After 2–3 weeks, the mice bearing tumors of about 1.0 cm diameter were selected for imaging. The free luciferin was dissolved in ethanol and other compounds were dissolved in dimethylsulfoxide (DMSO) as stock. Then they were diluted with saline to a final concentration of 3.75 mM (containing 0.5% Pluronic F-127). After being anesthetized with isoflurane, tumor-bearing nude mice were injected with 50  $\mu\text{L}$  of compounds in the tumor site. Then bioluminescence imaging was immediately performed with an exposure time of 60 s. The light signal was recorded every 5 min until it disappeared. The control group received an equal volume of saline only. Each compound was evaluated using at least three nude mice.

## Conclusions

In summary, the prodrug or caged-luciferin strategy affords an excellent platform for persistent bioluminescence imaging.<sup>45–51</sup> By introducing ester protecting groups of different sizes into the carbonyl group of the free luciferin, we designed and synthesized ten novel pro-substrates for *Renilla*

luciferase. These precursors could be effectively activated by intracellular esterases, lipases or nucleophilic substances, leading to a bioluminescence enhancement. After careful evaluation *in vitro*, *in cellulo* and *in vivo*, we found that butyryloxymethyl luciferin 7 with low cytotoxicity displayed prolonged bioluminescence imaging in living cells and mice. Therefore, this molecule can serve as a long-acting substrate for noninvasive extended bioluminescence imaging.

## Author contributions

M. L., L. D., I. Y., Y. H., M. Y. and X. M. designed the experiments. M. Y., T. J., Y. G., Y. C. and C. Z. synthesized the molecules. M. Y., X. M., X. Y. and Y. H. performed the biological evaluations of the molecules. M. L. and L. D. wrote the main manuscript text, and Y. H. and X. M. prepared all of the figures.

## Conflicts of interest

There are no conflicts to declare.

## Acknowledgements

This work was supported by grants from the National Program on Key Basic Research Project (no. 2013CB734000), the National Natural Science Foundation of China (no. 81673393), the Taishan Scholar Program at Shandong Province, the Qilu Scholar Program at Shandong University, the Shandong Provincial Natural Science Foundation (no. ZR2013HQ055), the American Cancer Society (no. RSG-16-215-01 TBE), the Russian Science Foundation (no. 17-14-01169) and the Major Project of Science and Technology of Shandong Province (no. 2015ZDJS04001).

## Notes and references

- 1 K. Pinel, J. Lacoste, G. Plane, M. Ventura and F. Couillaud, *Gene Ther.*, 2014, **21**, 434–439.
- 2 J. R. Pribaz, N. M. Bernthal, F. Billi, J. S. Cho, R. I. Ramos, Y. Guo, A. L. Cheung, K. P. Francis and L. S. Miller, *J. Orthop. Res.*, 2012, **30**, 335–340.
- 3 J. E. Kim, S. Kalimuthu and B. C. Ahn, *Nucl. Med. Mol. Imaging*, 2015, **49**, 3–10.
- 4 D. M. Yurek, A. M. Fletcher, M. McShane, T. H. Kowalczyk, L. Padegimas, M. R. Weatherspoon, M. D. Kaytor, M. J. Cooper and A. G. Ziady, *Mol. Imaging*, 2011, **10**, 327–339.
- 5 Y. Inoue, F. Sheng, S. Kiryu, M. Watanabe, H. Ratanakanit, K. Izawa, A. Tojo and K. Ohtomo, *Mol. Imaging*, 2011, **10**, 377–385.
- 6 J. Huang, Y. M. Li, Q. Cheng, D. A. Vallera and W. A. Hall, *Mol. Med. Rep.*, 2015, **12**, 5163–5168.





- 7 A. Dragulescu-Andrasi, C. T. Chan, A. De, T. F. Massoud and S. S. Gambhir, *Proc. Natl. Acad. Sci. U. S. A.*, 2011, **108**, 12060–12065.
- 8 W. X. Wu, J. Li, L. Z. Chen, Z. Ma, W. Zhang, Z. Z. Liu, Y. N. Cheng, L. P. Du and M. Y. Li, *Anal. Chem.*, 2014, **86**, 9800–9806.
- 9 X. D. Tian, Z. Y. Li, C. W. Lau and J. Z. Lu, *Anal. Chem.*, 2015, **87**, 11325–11331.
- 10 P. Feng, H. T. Zhang, Q. K. Deng, W. Liu, L. H. Yang, G. B. Li, G. Chen, L. P. Du, B. W. Ke and M. Y. Li, *Anal. Chem.*, 2016, **88**, 5610–5614.
- 11 D. M. Mofford, S. T. Adams, G. S. K. K. Reddy, G. R. Reddy and S. C. Miller, *J. Am. Chem. Soc.*, 2015, **137**, 8684–8687.
- 12 H. Takakura, R. Kojima, M. Kamiya, E. Kobayashi, T. Komatsu, T. Ueno, T. Terai, K. Hanaoka, T. Nagano and Y. Urano, *J. Am. Chem. Soc.*, 2015, **137**, 4010–4013.
- 13 Y. Yuan, F. Q. Wang, W. Tang, Z. L. Ding, L. Wang, L. L. Liang, Z. Zheng, H. F. Zhang and G. L. Liang, *ACS Nano*, 2016, **10**, 7147–7153.
- 14 Z. M. Kaskova, A. S. Tsarkova and I. V. Yampolsky, *Chem. Soc. Rev.*, 2016, **45**, 6048–6077.
- 15 J. Li, L. Chen, L. Du and M. Li, *Chem. Soc. Rev.*, 2013, **42**, 662–676.
- 16 W. W. Lorenz, R. O. McCann, M. Longiaru and M. J. Cormier, *Proc. Natl. Acad. Sci. U. S. A.*, 1991, **88**, 4438–4442.
- 17 E. P. Coutant and Y. L. Janin, *Chem. – Eur. J.*, 2015, **21**, 17158–17171.
- 18 T. Y. Jiang, L. P. Du and M. Y. Li, *Photochem. Photobiol. Sci.*, 2016, **15**, 466–480.
- 19 J. C. Woo, M. H. Howell and A. G. Von Arnim, *Protein Sci.*, 2008, **17**, 725–735.
- 20 S. Bhaumik and S. S. Gambhir, *Proc. Natl. Acad. Sci. U. S. A.*, 2002, **99**, 377–382.
- 21 H. Zhao, T. C. Doyle, R. J. Wong, Y. Cao, D. K. Stevenson, D. Piwnica-Worms and C. H. Contag, *Mol. Imaging*, 2004, **3**, 43–54.
- 22 K. D. G. Pflieger and K. A. Eidne, *Nat. Methods*, 2006, **3**, 165–174.
- 23 S. H. Sun, X. B. Yang, Y. Wang and X. H. Shen, *Int. J. Mol. Sci.*, 2016, **17**, 1704.
- 24 M. Paola, I. Casella and T. Costa, *Acta Pharmacol. Sin.*, 2006, **27**, 405–405.
- 25 L. Saleh and C. Plieth, *Nat. Protoc.*, 2010, **5**, 1635–1641.
- 26 Y. H. Jeon, S. A. Bae, Y. J. Lee, Y. L. Lee, S. W. Lee, G. S. Yoon, B. C. Ahn, J. H. Ha and J. Lee, *Mol. Imaging*, 2010, **9**, 343–350.
- 27 T. Kimura, K. Hiraoka, N. Kasahara and C. R. Logg, *J. Gene Med.*, 2010, **12**, 528–537.
- 28 L. Mezzanotte, M. Aswendt, A. Tennstaedt, R. Hoeben, M. Hoehn and C. Lowik, *Contrast Media Mol. Imaging*, 2013, **8**, 505–513.
- 29 L. J. Kricka, *Anal. Chem.*, 1993, **65**, R460–R462.
- 30 M. Mirasoli and E. Michelini, *Anal. Bioanal. Chem.*, 2014, **406**, 5529–5530.
- 31 N. Vassel, C. D. Cox, R. Naseem, V. Morse, R. T. Evans, R. L. Power, A. Brancale, K. T. Wann and A. K. Campbell, *Luminescence*, 2012, **27**, 234–241.
- 32 T. Y. Jiang, X. F. Yang, X. Y. Yang, M. L. Yuan, T. C. Zhang, H. T. Zhang and M. Y. Li, *Org. Biomol. Chem.*, 2016, **14**, 5272–5281.
- 33 J. Levi, A. De, Z. Cheng and S. S. Gambhir, *J. Am. Chem. Soc.*, 2007, **129**, 11900–11903.
- 34 M. Otto-Duessel, V. Khankaldyyan, I. Gonzalez-Gomez, M. C. Jensen, W. E. Laug and M. Rosol, *Mol. Imaging*, 2006, **5**, 57–64.
- 35 E. Lindberg, S. Mizukami, K. Ibata, A. Miyawaki and K. Kikuchi, *Chemistry*, 2013, **19**, 14970–14976.
- 36 M. Hattori, G. Kawamura, R. Kojima, M. Kamiya, Y. Urano and T. Ozawa, *Anal. Chem.*, 2016, **88**, 6231–6238.
- 37 Z. F. Walls, S. V. Gupta, G. L. Amidon and K. D. Lee, *Bioorg. Med. Chem. Lett.*, 2014, **24**, 4781–4783.
- 38 P. L. Meisenheimer, H. T. Uyeda, D. P. Ma, M. Sobol, M. G. McDougall, C. Corona, D. Simpson, D. H. Klaubert and J. J. Cali, *Drug Metab. Dispos.*, 2011, **39**, 2403–2410.
- 39 F. F. Craig, A. C. Simmonds, D. Watmore, F. Mccapra and M. R. H. White, *Biochem. J.*, 1991, **276**, 637–641.
- 40 M. Nakamura, T. Suzuki, N. Ishizaka, J. Sato and S. Inouye, *Tetrahedron*, 2014, **70**, 2161–2168.
- 41 M. L. Yuan, X. J. Ma, T. Y. Jiang, C. C. Zhang, H. Chen, Y. Q. Gao, X. Y. Yang, L. P. Du and M. Y. Li, *Org. Biomol. Chem.*, 2016, **14**, 10267–10274.
- 42 M. L. Yuan, T. Y. Jiang, L. P. Du and M. Y. Li, *Chin. Chem. Lett.*, 2016, **27**, 550–554.
- 43 G. Giuliani, A. Cappelli, S. Vomero and M. Anzini, *WO 2011007314*, 2011.
- 44 G. Giuliani, P. Molinari, G. Ferretti, A. Cappelli, M. Anzini, S. Vomero and T. Costa, *Tetrahedron Lett.*, 2012, **53**, 5114–5118.
- 45 L. Cui, Y. Zhong, W. P. Zhu, Y. F. Xu, Q. S. Du, X. Wang, X. H. Qian and Y. Xiao, *Org. Lett.*, 2011, **13**, 928–931.
- 46 Y. Cheng, F. Huang, X. Min, P. Gao, T. Zhang, X. Li, B. Liu, Y. Hong, X. Lou and F. Xia, *Anal. Chem.*, 2016, **88**, 8913–8919.
- 47 M. Bio, P. Rajaputra, G. Nkepan and Y. J. You, *J. Med. Chem.*, 2014, **57**, 3401–3409.
- 48 F. Kong, Z. Liang, D. Luan, X. Liu, K. Xu and B. Tang, *Anal. Chem.*, 2016, **88**, 6450–6456.
- 49 H. Seki, S. Xue, S. Pellet, P. Silhar, E. A. Johnson and K. D. Janda, *J. Am. Chem. Soc.*, 2016, **138**, 5568–5575.
- 50 W. Hakamata, S. Tamura, T. Hirano and T. Nishio, *ACS Med. Chem. Lett.*, 2014, **5**, 321–325.
- 51 C. Perez, K. B. Daniel and S. M. Cohen, *ChemMedChem*, 2013, **8**, 1662–1667.

